Link Budget Evaluation Scheme for UWB Transmission Systems

Sathaporn Promwong[†,††], and Jun-ichi Takada[†]
[†]Graduate School of Science and Engineering, Tokyo Institute of Technology
O-okayama Minami 6 Bldg., 2–12–1, O-okayama, Meguro-ku, 152–8550, Tokyo, Japan.
[††]Department of Information Engineering, Faculty of Engineering,
King Mongkut's Institute of Technology Ladkrabang, Bangkok 10520, Thailand.
E-mail: kpsathap@kmitl.ac.th

***Abstract*— This paper present the link budget evaluation scheme for UWB system based on the extended Friis' transmission formula. The template waveform is considered at the receiver side to maximize the SNR for evaluation. An experimental evaluation of the antenna transfer function needs the three types of broadband antennas. The technique gives very accurate results and is very useful for design and evaluation of UWB impulse radio transmission systems, especially for the evaluation of waveform distortion effects.**

Keywords: UWB, link budget, impulse radio, Friis' transmission formula

I. Introduction

Ultra wideband (UWB) communication systems, the antennas are signi cantly pulse-shaping lters. Any distortion of the signal in the frequency domain causes the distortion of the transmitting pulse shape. Consequently this will increase the complexity of the detection mechanism at the receiver [1]. Moreover, low cost, geometrically small and still ef cient structures are required for typical wireless applications. Therefore the antenna design for UWB signal radiation is one of the main challenges [2], [3].

Even if the channel is in line of sight (LOS), Friis' transmission formula cannot be directly applied to the UWB radio as the bandwidth of the pulse is extremely wide. Furthermore, simple comparison between waveforms of transmitter and receiver is not signi cant because of the distortion of the waveform caused by the frequency response of the antenna.

In this paper, we discuss the free space link budget evaluation scheme for UWB impulse radio systems. This scheme is based on the Friis' transmission formula, adapted for UWB, in the sense that we would like to derive the equivalent antenna gain for UWB impulse radio systems. The transmission waveform and the receiver template waveform are keys for the extension of the Friis' transmission formula to UWB system. An experiment is carried out using three types of broadband antennas for UWB operation in the anechoic chamber.

II. Thoery

In this study, we focus on the link budget evaluation for UWB impulse radio system in free space.

A. Extension of Friis' Transmission Formula for UWB transmission System

In narrowband systems, the link budget of the free space propagation loss is usually estimated by using Friis' transmission formula [4]. However, it is not directly applicable to the UWB impulse radio transmission system, as the formula is expressed as a function of the frequency. Moreover, the waveform may be distorted due to the frequency characteristics of the antenna. Ref. [5] treats the special cases of the constant gain and the constant aperture, but no general discussion had been made although it suggested the use of the time-domain antenna effective length.

The Friis' transmission formula [4] has been widely used, and can be applied to the calculation of these LOS channels.

$$G_{\text{Friis}}(f) = \frac{P_{\text{r}}(f)}{P_{\text{t}}(f)} = G_{\text{f}}(f)G_{\text{r}}(f)G_{\text{t}}(f), \tag{1}$$

where G_{r} and G_{t} are Rx and Tx antenna gain,

$$G_{\text{f}}(f) = \left(\frac{\lambda}{4\pi d}\right)^2 \tag{2}$$

is the free space propagation gain (less than unity in practice), $\lambda = \frac{c}{f}$ is the wavelength, c is the velocity of the light, f is the operating frequency, and d is the separation between transmitter and receiver antennas.

It is noted, however, that Eq. (1) is satis ed only at some certain frequency, and is not directly applicable to UWB systems. The Friis' transmission formula shall

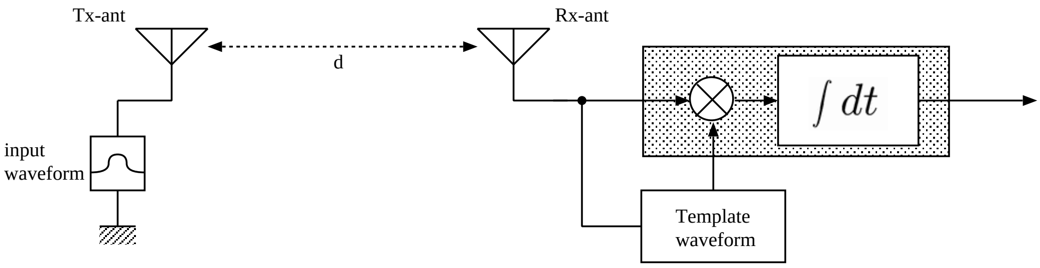

Fig. 1. Block diagram of transmission system for UWB signal.

be extended to take into account the transmission signal waveform and its distortion as well [6], [7].

Input signal $v_\mathrm{i}(t)$ at the transmitter port is expressed as the convolution of an impulse input and the pulse shaping lter $h_\mathrm{i}(t)$ as

$$v_\mathrm{i}(t) = E_\mathrm{i}\delta(t) * h_\mathrm{i}(t), \tag{3}$$

where

$$\int_{-\infty}^{\infty} h_\mathrm{i}^2(t)\mathrm{d}t = \int_{-\infty}^{\infty} |H_\mathrm{i}(f)|^2 \,\mathrm{d}f = 1. \tag{4}$$

Friis' formula is extended taking into account the transmission waveform as

$$H_\text{e-Friis}(f) = \frac{V_\mathrm{r}(f)}{E_\mathrm{i}} = H_\mathrm{f} H_\mathrm{i} \mathbf{H}_\mathrm{r} \cdot \mathbf{H}_\mathrm{t}, \tag{5}$$

where

$$\begin{aligned} \mathbf{H}_a &= \mathbf{H}_a(\theta_a,\ \varphi_a,\ f) \\ &= \hat{\boldsymbol{\theta}}_a H_{a\theta}(\theta_a,\ \varphi_a,\ f) + \hat{\boldsymbol{\varphi}}_a H_{a\varphi}(\theta_a,\ \varphi_a,\ f), \qquad (6) \\ a &= \mathrm{r}\ \textit{or}\ \mathrm{t}, \end{aligned}$$

is a complex transfer function vector of the antenna relative to the isotropic antenna,

$$H_\mathrm{f} = \frac{\lambda}{4\pi d}\exp(-\mathrm{j}kd), \tag{7}$$

is the free space transfer function where

$$k = \frac{2\pi}{\lambda}, \tag{8}$$

is the propagation constant.

B. Correlation Receiver

Let us consider a correlation receiver shown in Fig. 1. The output SNR is dependent on the choice of the template waveform. The correlator output $v_\mathrm{o}(\tau)$ is therefore expressed as

$$v_\mathrm{o}(\tau) = \int_{-\infty}^{\infty} v_\mathrm{r}(t) h_\mathrm{w}(t-\tau)\mathrm{d}t, \tag{9}$$

where $v_\mathrm{r}(t)$ is the receiver input waveform which is inverse Fourier transform, and $h_\mathrm{w}(t)$ is the template waveform. τ corresponds to the timing of the template waveform, and the optimum timing τ_o is chosen as

$$\tau_\mathrm{o} = \arg\max_{\tau} v_\mathrm{o}(\tau). \tag{10}$$

Hereafter $h_\mathrm{w}(t)$ is normalized as

$$\int_{-\infty}^{\infty} |h_\mathrm{w}(t)|^2 \mathrm{d}t = 2B, \tag{11}$$

where B is the signal bandwidth, so that the output noise power is constant as $N_0 B$, where $\frac{N_\mathrm{o}}{2}$ is power spectral density of AWGN.

Under the constraint of Eq. (11), $h_\mathrm{wm}(t)$ maximizes $v_\mathrm{o}(\tau_\mathrm{o})$ when $h_\mathrm{wm}(t)$ is a time-reversed and scaled version of $v_\mathrm{r}(t)$, i.e.

$$h_\mathrm{wm}(t) = \frac{\sqrt{2B}\, v_\mathrm{r}(\tau_\mathrm{o} - t)}{\sqrt{\int_{-\infty}^{\infty} |v_\mathrm{r}(t)|^2 \mathrm{d}t}}, \tag{12}$$

where τ_o is usually chosen so that $h_\mathrm{wm}(t) = 0$ for $t < 0$ to satisfy the causality. $h_\mathrm{wm}(t)$ is called the optimum template waveform hereafter. It is noted that the link budget evaluation is identical to that in Ref. [10] when $h_\mathrm{wm}(t)$ is used as the receiver template.

C. Isotropic Correlation Receiver

It is obvious from Eq. (12) that the optimum template waveform is not the simple time-reversed version of the transmitter waveform, but the channel characteristics including the antennas and the free space propagation. Therefore, it is not always feasible to adapt the template waveform to the angular-dependent antenna characteristics, since the waveform shall be generated at the clock rate of tens of gigahertz. Therefore, we consider a canonical template waveform $h_\mathrm{wc}(t)$. In this paper we have chosen $h_\mathrm{wc}(t)$ that is optimum for the isotropic and the constant gain antennas, i.e.

$$h_\mathrm{wc}(t) = \frac{\sqrt{2B}\, v_\text{r-iso}(\tau_\mathrm{o} - t)}{\sqrt{\int_{-\infty}^{\infty} |v_\text{r-iso}(t)|^2 \mathrm{d}t}}, \tag{13}$$

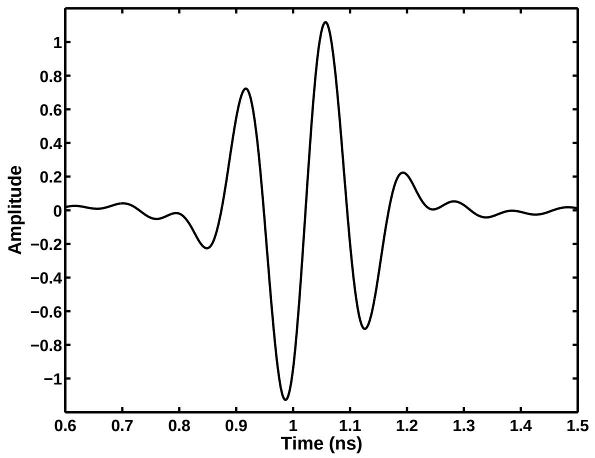

Fig. 2. The transmission waveform of UWB signal.

where

$$v_{\text{r-iso}}(t) = \int_{-\infty}^{\infty} H_{\text{f}}(f) V_{\text{t}}(f) \exp(\text{j}2\pi f t)\text{d}f \qquad (14)$$

is the receiver input voltage for isotropic antenna including. The difference between the optimum and the isotropic templates indicates quantitatively the distortion of the waveform.

III. Measurement of Antenna Transfer Function

A. UWB waveform Transmission

The effect of the waveform distortion is more obvious when the bandwidth is wider. We considered the impulse radio signal that fully covers the FCC band [8], i.e., $3.1 \sim 10.6$ GHz. The center frequency and the bandwidth were therefore set to be $f_0 = 6.85$ GHz and $f_{\text{b}} = 7.5$ GHz, respectively. The transmit waveform assumed in the simulation was a single ASK pulse with the carrier frequency f_0. To satisfy the bandwidth requirement of f_{b}, the pulse length was set to be $\frac{2}{f_{\text{b}}}$. Then the signal was band-limited by a Nyquist roll-off lter with roll-off factor $\alpha = 0$ (rectangular window) and passband $\left(f_0 - \frac{f_{\text{b}}}{2},\ f_0 + \frac{f_{\text{b}}}{2}\right)$. Figure 2 shows the transmit pulse waveform. The transmission process of the pulse waveform is simulated based on the measured transfer function of the antenna.

B. Experimental Setup and Measurement Model

The VNA was operated in the response measurement mode, where Port-1 was the transmitter port (Tx) and Port-2 was the receiver port (Rx), respectively. Biconical antennas with the maximum diameter of 65.3 mm and the length of 37 mm are used both as the standard antennas and as AUT [9]. The measurement was done in the anechoic chamber. Both Tx and Rx antennas were x ed at the height of 1.75 m and separated at a distance of 4 m. The setup is sketched in Fig. 3.

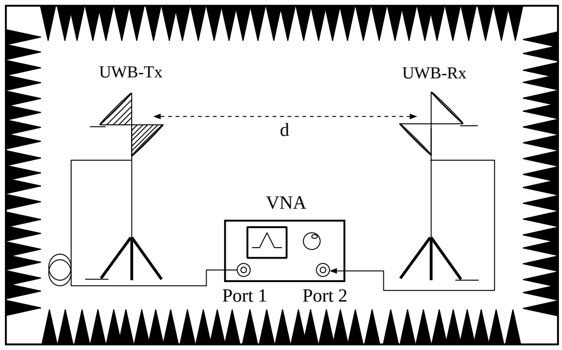

Fig. 3. The instrument setup.

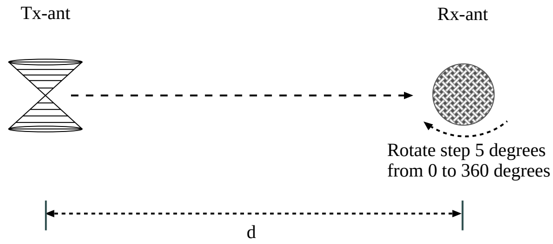

Fig. 4. Top view antenna setting.

Figure 4 shows the orientations of the S_{21}, transfer function measurement for Tx and Rx antennas. The Tx antenna is x ed at pointing angle $0°$ and the Rx antenna is rotated from pointing angle $0°$ to $360°$ with each step at $5°$.

C. Parameters of Experiment and Calibration Techniques

The important parameters for the experiments are listed in Table I.

It is noted that the calibration is done at the connectors of the cables to be connected to the antennas. Therefore, all the impairments of the antenna characteristics are included in the measured results.

IV. Results

In this section, standard broadband antennas and deployable antennas are used in the measurement for the link budget evaluation.

USA suggested the use of a biconical antenna, and log-periodic antenna for the frequency ranges of $30 - 200$ MHz, $200 - 960$ MHz, and $0.96 - 18$ GHz, respectively, for the compliance test of UWB transmitters [11].

TABLE I

EXPERIMENTAL SETUP PARAMETERS.

Parameter	Value
Frequency range	3 GHz to 11 GHz
Number of frequency points	1601
Dynamic power range	80 dB
Tx antenna height	1.75 m
Rx antenna height	1.75 m
Distance between Tx and Rx	4 m
Rx rotate range	$0°$ to $360°$
Rx rotate step	$5°$

We chose these two kinds of antennas, operating in the same frequency range.

1) Biconical Antenna: First, the same biconical antennas were used at both Tx and Rx sides. Figure 6 shows the normalized UWB transmission gain as a function of antenna pointing angle in E-plane. Well-known 8-shaped patterns were obtained. Two template waveforms were used for comparison, and the difference was rather small. The phase center of the biconical antenna is the feed point and it has theoretically the frequency independent gain at the broadside direction, and that is why the waveform distortion effect is small compared with the isotropic template.

2) Log-Periodic Dipole Antenna: A log-periodic dipole antenna (LPDA) is also used for the broadband use. It has also a frequency-independent gain. Different from biconical antennas, however, the dispersion characteristic of LPDA is rather big, since the phase center changes by the frequency due to the resonance of the dipole elements [12].

We used a commercial LPDA, Watkins–Johnson's AR7-15A, shown in Fig. 7. The antenna has been designed to operate in the range of 1 to 12.4 GHz. Figure 8 shows the normalized UWB transmission gain pattern for biconical–LPDA link in E-plane. As is known, an LPDA is uni-directional and its gain is higher than that of a biconical antenna. The degradation of the transmission gain is observed when the canonical isotropic template is used, since the waveform dispersion is obvious [12].

3) Meander Line Miniature Antenna: Among many types of UWB miniature antennas, SkyCross' SMT-3TO10M-A meander line antenna (MLA) has been a rst commercial product [13]. It is as small as $16\times13.6\times3$ mm and operates at the frequency range from 3.1 to 10 GHz. The detailed structure is not presented, but the related patents show that it is a transmission line type antenna and the meander line operates as the slow wave structure to reduce the size [14].

Figure 10 shows the normalized UWB transmission gain pattern for biconical–MLA link in E-plane. Note that $0°$ and $90°$ are the broadside and the feed of the antenna, respectively. Therefore, the beam direction was tilted toward the upper direction. The transmission gain is about the same as the isotropic link. Since the size is very small, the phase center is unchanged. Therefore, the results for the isotropic template and the ideal template are not so different.

V. CONCLUSION

This paper the link budget evaluation scheme for UWB transmission gain, which includes the transmit waveform, the antennas, free space propagation, and the receiver correlator template. By using the de nition, we have evaluated three types of broadband antennas. This scheme may be effective especially to evaluate the deployable antenna with non-ideal frequency characteristics of the return loss and the directivity, as the overall performance can be evaluated only by the UWB transmission gain.

REFERENCES

[1] K. Siwiak, "Impact of ultra wide band transmissions on a generic receiver," Proc. 2001 Spring IEEE Veh. Tech. Conf. (VTC), Rhodes, Greece, vol. 2, pp. 1181–1183, May 2001.

[2] H.F. Harmuth and S. Ding-Rong, "Antennas for Nonsinusiodal Wave — Part I: Radiators," IEEE Trans. Elec. Mag. Compat., vol. EMC-25, no. 1, pp. 13–24, Feb. 1983.

[3] H.F. Harmuth and S. Ding-Rong, "Antennas for Nonsinusiodal Wave — Part II: Sensors," IEEE Trans. on Elec. Mag. Compat., vol. EMC-25, no. 1, no. 2, pp. 107–115, May 1983.

[4] H.T. Friis, "A note on a simple transmission formula," Proc. IRE, vol. 34, no. 5, pp. 254–256, May 1946.

[5] United States of America, "Path loss calculations for ultra-wideband signals in indoor environments," ITU-R Document 3K/30-E, pp. 1–14, Nov. 2003.

[6] J. Takada, S. Promwong and W. Hachitani, "Extension of Friis' Transmission Formula for Ultra-Wideband Systems," IEICE Tech. Rep., WBS2003-8/MW2003-20, May 2003.

[7] A.H. Mohammadian, A. Rajkotia, and S.S. Soliman, "Characterization of UWB Transmit-Receive Antenna System," Proc. IEEE Conf. Ultra Wideband Syst. Tech. (UWBST) 2003, Nov. 2003.

[8] Federal Communications Commission, "Revision of Part 15 of the Commission's Rules Regarding Ultra-Wideband Transmission Systems," First Report and Order, FCC 02–48, Apr. 2002.

[9] S. Promwong, W. Hachitani, J. Takada, P. Supanakoon, and P. Tangtisanon "Experimental Study of Ultra-Wideband Transmission Based on Friis' Transmission Formula," The Third International Symposium on Communications and Information Technology (ISCIT) 2003, vol. 1. pp. 467–470, Sept. 2003.

[10] S. Promwong, and J. Takada, "Free space link budget estimation scheme for ultra wideband impulse radio with imperfect antennas," IEICE Electronics Express, vol. 1, no. 7, pp. 188–192, July 2004.

[11] United States of America, "Working document towards the development of measurement procedures for assessing regulatory compliance of ultra-wideband emitters," ITU-R Document, 1-8/157-E, June 2004.

[12] H.G. Schantz, "Dispersion and UWB antennas," Proc. 2004 Int. Workshop Ultra Wideband Syst. / Conf. Ultra Wideband Syst. Tech. (Joint UWBST & IWUWBS 2004), Kyoto, Japan, May 2004.

[13] Skycross Inc., "3.1 – 10 GHz UWB Antenna for Commercial UWB Applications," `http://www.skycross.com/`

[14] "Wideband meander line loaded antenna," U.S. Patent 6,492,953 B2, Dec. 2002.

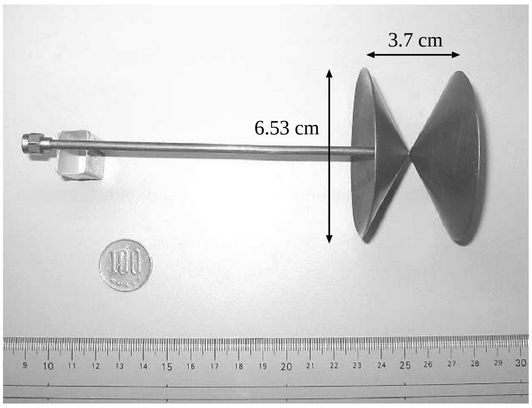

Fig. 5. Biconical antenna structure.

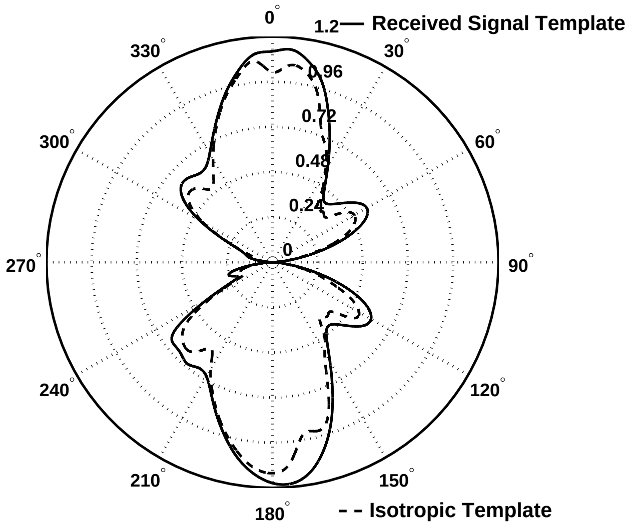

Fig. 6. Normalized UWB transmission gain for biconical–biconical link.

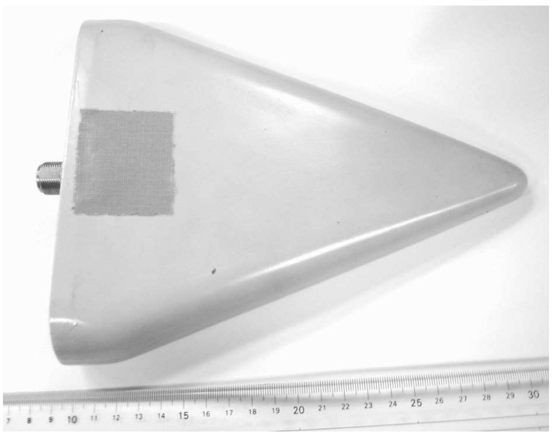

Fig. 7. Log-periodic dipole antenna (Watkins–Johnson AR7-15A).

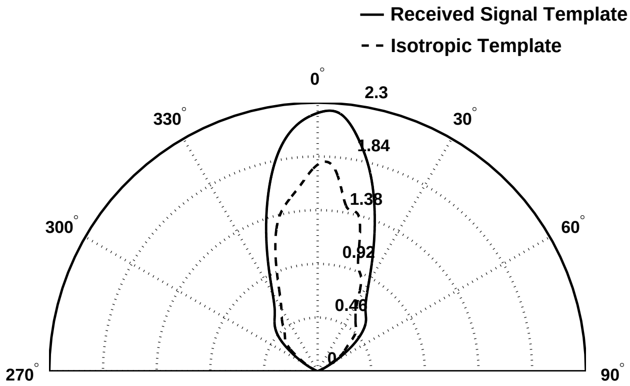

Fig. 8. Normalized UWB transmission gain for biconical–LPDA link.

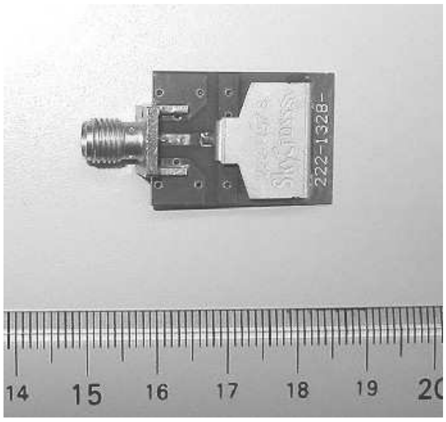

Fig. 9. Meander line antenna (SkyCross' SMT-3TO10M-A).

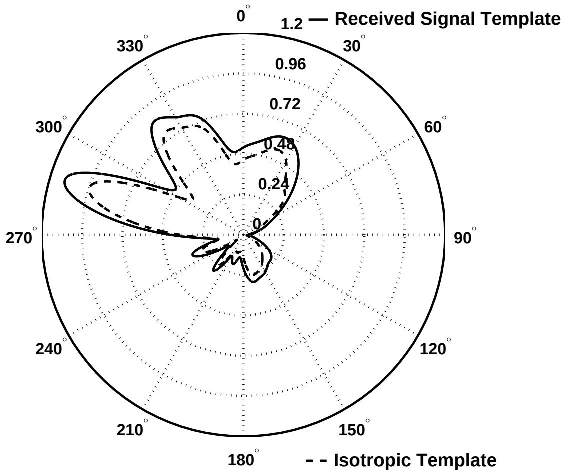

Fig. 10. Normalized UWB transmission gain for biconical–MLA link.